Decoherence induced by hyperfine interactions with nuclear spins in antiferromagnetic molecular rings

F. Troiani,* V. Bellini, and M. Affronte

CNR-INFM–National Research Center on Nano-Structures and Bio-Systems at Surfaces (S^3), Via Campi 213/A, 41100 Modena, Italy and Dipartimento di Fisica, Università degli Studi di Modena e Reggio Emilia, Via Campi 213/A, 41100 Modena, Italy

(Received 28 November 2007; published 21 February 2008)

Molecular magnets are effective few-level spin systems that allow for the observation of coherent dynamics. Electronic coherence is mainly limited by hyperfine interactions with nuclear spins. Here, we theoretically investigate the resulting inhomogeneous broadening and electron-nuclear entanglement: They take place on the nanosecond and microsecond time scales, respectively. Our microscopic description allows us to clarify the role played by the different chemical elements. The effect of spin echo and the dependence of decoherence on the magnetic field are also estimated.

DOI: 10.1103/PhysRevB.77.054428 PACS number(s): 75.50.Xx, 03.65.Yz, 03.67.Lx

I. INTRODUCTION

In an open system ($\mathcal{S}$), linear superpositions between quantum states are made fragile by the possible entanglement between $\mathcal{S}$ and the environment ($\mathcal{E}$). Such phenomenon, known as *decoherence*, is believed to lie at the heart of the quantum-classical transition and of the measurement problem.[1–3] Decoherence also represents a key issue from a technological point of view. In fact, the extra potentialities of quantum-information devices with respect to classical ones rely also on a massive exploitation of linear superpositions and of the resulting quantum interference.[4] In both the fundamental and technological perspectives, the localized electron interacting with a spin bath plays a special role: On the one hand, it represents a paradigmatic case of non-Markovian decoherence;[5] on the other hand, it is one of the most investigated systems in view of a solid-state implementation of quantum-information processing.[6–8]

Since a decade ago, great attention is devoted to electron spins localized in low-dimensional semiconductor heterostructures. Molecular antiferromagnets were recently recognized as alternative implementations of effective few-level spin systems, where coherent dynamics and perform quantum gates can be observed.[9,10] Relevant to this aim is that both the electronic properties and the nuclear environment can be selectively modified by means of chemical synthesis.[11] Besides, the development of extremely sensitive magnetometers[12] and of novel procedures for grafting molecules on selected portions of patterned surfaces[13,14] paves the way to the manipulation and detection of individual nanomagnets.

The present paper is specifically concerned with the effects of hyperfine interactions on the electronic coherence of a heterometallic antiferromagnetic ring, namely, Cr_7Ni.[11] These molecules possess a number of appealing features for the encoding and manipulation of quantum information,[15,16] and are being widely investigated by different experimental techniques.[35] In the parent molecule Cr_8, electron-nuclear coupling was exploited as a means for locally probing the spin-moment distribution.[17] As to the dynamical properties, the electron-spin decoherence time was recently measured in spin-echo experiments.[18] In molecular arrays or crystals, a major contribution to decoherence arises from intermolecular dipole-dipole interactions between electron spins.[19] While these can be possibly reduced by dilution, spin coherence is ultimately limited by hyperfine interactions: These represent an intrinsic source of decoherence, which is still effective at the single-molecule level.

The paper is organized as follows: In Sec. II, we introduce the expressions that we use to quantify decoherence; in Sec. III, we define the effective Hamiltonian that accounts for the relevant dynamics of the nuclear spins; in Secs. IV and V, we show the effects of inhomogeneous broadening and nuclear flip-flop transitions, respectively; in Sec. VI, we discuss the effect of spin echo; in Sec. VII, we finally draw the conclusions.

II. DECOHERENCE

The energy spectrum of Cr_7Ni is characterized by the presence of a well resolved ground-state doublet ($S=1/2$, with S as the total electronic spin of the molecule), separated from the higher levels by a gap $\Delta \simeq 13$ K. Therefore, under the proper experimental and manipulation conditions, the molecule can be regarded as an effective two-level system, with the relevant subspace spanned by the states $|\Uparrow\rangle \simeq |S=1/2, M=1/2\rangle$ and $|\Downarrow\rangle \simeq |S=1/2, M=-1/2\rangle$ (with M as the total spin projection in the z direction, orthogonal to the molecule plane).[15] There, the molecule state is defined by the reduced density matrix $\rho_S = |c_\Downarrow|^2 |\Downarrow\rangle\langle\Downarrow| + |c_\Uparrow|^2 |\Uparrow\rangle\langle\Uparrow| + c_\Downarrow^* c_\Uparrow r(t) |\Uparrow\rangle\langle\Downarrow| + c_\Uparrow^* c_\Downarrow r^*(t) |\Downarrow\rangle\langle\Uparrow|$, obtained by tracing over the environment (i.e., nuclear-bath) degrees of freedom: $\rho_S = \mathrm{Tr}_\mathcal{E}\{\rho_{S\mathcal{E}}\}$. The key quantity to our present purposes is represented by the so-called *decoherence factor* $r(t)$, which quantifies the degree of purity of the molecule state. We assume $\rho_{S\mathcal{E}}$ to be initially factorized, and the system to be initialized in a pure state: $\rho_{S\mathcal{E}}(0) = |\psi_S\rangle\langle\psi_S| \otimes \rho_\mathcal{E}(0)$, where $|\psi_S\rangle = c_\Downarrow |\Downarrow\rangle + c_\Uparrow |\Uparrow\rangle$ and $\rho_\mathcal{E}(0) = \sum_{\alpha=1}^{N_\mathcal{E}} p_\alpha |\mathbf{I}_\alpha\rangle\langle\mathbf{I}_\alpha|$. Here, the $N_\mathcal{E}$ nuclear-spin configurations $|\mathbf{I}_\alpha\rangle \equiv \otimes_{p=1}^{N_n} |I_p^z(\alpha)\rangle$ span the Hilbert space corresponding to the $N_n = 152$ magnetic nuclei, with $I_p = I_\mathrm{H}, I_\mathrm{F}, I_\mathrm{Cr}$ (Fig. 1). In the pure-dephasing limit, the interaction between electronic and nuclear spins does not modify $|c_\Uparrow|$ and $|c_\Downarrow|$, thus leaving unaffected the diagonal

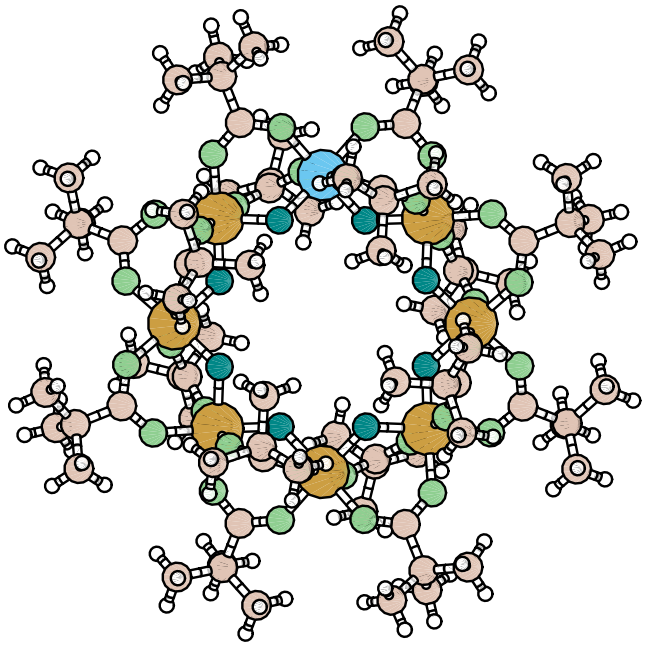

FIG. 1. (Color online) Molecular structure of the Cr_7Ni molecule (Ref. 11). The magnetic ions, Cr (orange) and Ni (cyan), form a quasiplanar octahedron. The molecule also includes: 8 F (blue), 32 O (green), 80 C (pink), and 144 H atoms (white). Unless differently specified, only H and F are taken to possess a finite nuclear spin ($I_H=I_F=1/2$). Below, we also consider the ^{53}Cr isotope ($I_{Cr}=3/2$, with natural abundance if 9.5%).

terms in ρ_S. The state of the electronic spin, however, does affect the dynamics of the nuclei,

$$|\eta\rangle \otimes |\mathbf{I}_\alpha\rangle \rightarrow |\eta\rangle \otimes |\mathbf{I}_\alpha^\eta(t)\rangle (\ \eta = \Uparrow, \Downarrow).$$

This results in a system-environment entanglement, quantified by $r_\alpha(t)=\langle \mathbf{I}_\alpha^{\Downarrow}(t)|\mathbf{I}_\alpha^{\Uparrow}(t)\rangle$, and therefore results in a loss of the electronic coherence even in the case where the nuclei are initialized in a specific configuration $|\mathbf{I}_\alpha\rangle$. In the general case, $\rho_{\mathcal{E}}(0)$ corresponds to a (proper or improper) mixture of different states. Therefore, $r(t)=\Sigma_{\alpha=1}^{N_{\mathcal{E}}} p_\alpha r_\alpha(t)$ decays also in the absence of nuclear-spin flips $[|\langle \mathbf{I}_\alpha^\eta(t)|\mathbf{I}_\alpha\rangle|=1$, with $\eta=\Uparrow,\Downarrow]$. In fact, different nuclear states $|\mathbf{I}_\alpha\rangle$ result in different values of the Overhauser field and, therefore, in different phases $\arg\{r_\alpha(t)\}$. As discussed in the following, these two effects are characterized by different time scales and can be, to a large extent, discussed separately.

III. EFFECTIVE SPIN HAMILTONIAN

Starting from a microscopic description of the molecule and its environment, we model the overall system in terms of an electron-nuclear spin Hamiltonian H. In a first step, the Hamiltonian H_e involving only the electron-spin degrees of freedom is diagonalized to derive the eigenstates $|\Uparrow\rangle$ and $|\Downarrow\rangle$.[15] H_e accounts for the Heisenberg and the dipole-dipole interactions between the $N_e=8$ magnetic ions $\mathbf{s}_p$ ($s_{Cr}=3/2$, $s_{Ni}=1$), as well as for their coupling to local crystal field and external magnetic field $\mathbf{B}$. The eigenstates of H_e typically present a high degree of correlation between the individual ion states, resulting from the mixing of different configurations: $|\eta\rangle=\Sigma_\alpha c_\alpha^\eta|\mathbf{S}_\alpha\rangle$, with $|\mathbf{S}_\alpha\rangle \equiv \otimes_{p=1}^{N_e}|s_p^z(\alpha)\rangle$ and $\eta=\Uparrow,\Downarrow$. These eigenstates determine the effective coupling constants between electron and nuclear spins, within the subspace corresponding to the ground-state doublet (see below).

The nuclear part, which includes both the Zeeman and the dipole-dipole interaction terms, reads $H_n=H_n^Z+H_{nn}^{dip}=\Sigma_{p=1}^{N_n}\omega_p^n I_p^z+\Sigma_{p<q}h_{nn}^{dip}(\mathbf{I}_p,\mathbf{I}_q)$. Finally, the electron-nuclear hyperfine interactions include both the Fermi-contact and the dipole-dipole contributions:

$$H_{en}=H_{en}^{dip}+H_{en}^c=\sum_{p=1}^{N_e}\sum_{q=1}^{N_n} h_{en}^{dip}(\mathbf{s}_p,\mathbf{I}_q) + \sum_{p=1}^{N_n}(a_p/2)\mathbf{I}_p\cdot\sigma^{\mathcal{S}},$$

where $a_p=-\gamma_p^n B_p^{hyp}$ and $\sigma_{x,y,z}^{\mathcal{S}}$ are the Pauli matrices in the $\{|\Uparrow\rangle,|\Downarrow\rangle\}$ basis. The estimate of the hyperfine field B_p^{hyp} requires the knowledge of the electron-spin density corresponding to the molecule ground state. This is provided by *ab initio* density functional calculations.[20] The major contribution to B_p^{hyp} arises from the contact term given by the Breit formula for scalar-relativistic electrons,[21] and is proportional to the spin density averaged within a sphere of Thomson radius around the nucleus. In $3d$ magnetic atoms, s valence and core orbitals hybridize differently with the spin-polarized d states. In fact, their respective contributions to the contact field are oriented parallel and antiparallel to the spin moment. Since core polarization is more effective near the nucleus than the valence one, in the absence of transferred valence hyperfine field from neighboring magnetic atoms, the total hyperfine field is negative (i.e., opposite to the electronic spin moment).[22] Orbital and dipolar intra-atomic terms are generally small for a nearly tetragonal coordination and can be safely neglected. In our calculations, the contact field amounts to approximately -25 and -18 T for the Cr^{3+} and Ni^{2+} ions, respectively.

The natural basis for expressing the dipolar interaction H_{en}^{dip} is that of the electron-spin configurations $|s_p^z(\alpha)\rangle$. However, the relevant states to our present purposes are $|\Uparrow\rangle$ and $|\Downarrow\rangle$. Therefore, we express the single-spin operators in terms of the molecule eigenstates and project them onto the ground-state doublet subspace,

$$s_p^z \rightarrow \mathbb{P}_{1/2}s_p^z\mathbb{P}_{1/2}=\langle\Uparrow|s_p^z|\Uparrow\rangle\sigma_z^{\mathcal{S}},$$

$$s_p^{\pm} \rightarrow \mathbb{P}_{1/2}s_p^{\pm}\mathbb{P}_{1/2}=\langle\Uparrow|s_p^+|\Downarrow\rangle\sigma_{\pm}^{\mathcal{S}},$$

where $\sigma_-^{\mathcal{S}}=|\Downarrow\rangle\langle\Uparrow|$, $\sigma_+^{\mathcal{S}}=|\Uparrow\rangle\langle\Downarrow|$, and $\mathbb{P}_{1/2}=|\Uparrow\rangle\langle\Uparrow|+|\Downarrow\rangle\langle\Downarrow|$. After the above substitutions, the expression of H_{en}^{dip} becomes formally similar to that of a single 1/2 electron spin: $H_{en}^{dip}=\Sigma_{p=1}^{N_n}\Sigma_{\mu,\nu=\pm,z}D_p^{\mu\nu}\sigma_\mu^{\mathcal{S}}I_p^\nu$, where the composite character of the electronic spin is enclosed in the expectation values of the individual spins s_p. The coupling to the magnetic field is accounted by the effective Zeeman term, $H_e=(\Omega/2)\sigma_z^{\mathcal{S}}$. For further details on the above derivation, the reader is referred to Appendix A.

TABLE I. Maximum values (in neV) of the nuclear-nuclear interaction terms in $H_n^{(i,e)}$ and the relative chemical elements. The values refer to a molecule with or without a Cr isotope, with $B=1$ T.

I	$A_{\max}^{(i)}$	$B_{\max}^{(i)}$	$A_{\max}^{(e)}$	$B_{\max}^{(e)}$	$\omega_{\max}^{(e)}$
0	0.0122	0.0489	0.0183	0.0249	10.8
	(H-H)	(H-H)	(F-F)	(F-F)	(F)
3/2	0.0122	0.0489	0.0353	6.13	236
	(H-H)	(H-H)	(Cr-Cr)	(Cr-Cr)	(Cr)

For strong enough magnetic fields ($\Omega \gg D_p^{\mu\nu}, a_p$), real transitions between $|\Uparrow\rangle$ and $|\Downarrow\rangle$ are forbidden by energy conservation. Virtual electronic transitions are, however, effective and contribute to the nuclear flip-flop processes that are responsible for the nuclear dynamics.[23,24] This warrants the elimination in the lowest order of the terms that are off-diagonal in $\mathcal{S}$ by means of a suitable canonical transformation, $H'=e^{S}He^{-S}$, where $S=\Sigma_{p=1}^{N_n} S_p$ and

$$S_p = \frac{a_p + D_p^{+-}}{\Omega - \omega_p}\sigma_+^{\mathcal{S}} I_p^- + \frac{D_p^{++}}{\Omega + \omega_p}\sigma_+^{\mathcal{S}} I_p^+ + \frac{D_p^{+z}}{\Omega}\sigma_+^{\mathcal{S}} I_p^z - \text{H.c.}$$

The expressions of the coefficients $D_p^{\pm\xi}$ ($\xi=\pm, z$) are given in Appendix A. In H', we keep only the terms up to first order in $1/\Omega$ and the off-diagonal nuclear ones that conserve the z component of the total spin. As a result, the nuclear dynamics is induced by extrinsic transitions (e) that involve virtual transitions between the eigenstates of H_e and intrinsic ones (i), which are independent of the electron-spin state: $H'=(\Omega^r/2)\sigma_z^{\mathcal{S}}+H_n^{(i)}+\sigma_z^{\mathcal{S}}\otimes H_n^{(e)}$,[25,26] where

$$H_n^{(\chi)} = \sum_{p=1}^{N_n} \omega_p^{(\chi)} I_p^z + \sum_{p\neq q} A_{p,q}^{(\chi)} I_p^+ I_q^- + \sum_{p\leqslant q} B_{p,q}^{(\chi)} I_p^z I_q^z, \qquad (1)$$

with $\chi=i,e$ (for the expressions of the coefficients that enter the above Hamiltonian, see Appendix B). The electron and nuclear Zeeman splittings, Ω^r and $\omega_p^{(i)}$, are renormalized by the mutual interaction. In $H_n^{(e)}$, the first term corresponds to an Ising coupling between electron and nuclear spins. The second and third ones account for the nuclear flip-flop processes and Ising interaction, respectively; both are mediated by a virtual transition of the electronic spin. Accordingly, the coefficients $A_{p,q}^{(e)}$ and $B_{p,q}^{(e)}$ are inversely proportional to the electronic Zeeman splitting Ω. No such dependence is present in $H_n^{(i)}$, which includes terms from H_n.

The nuclear dynamics is finally computed within the pair-correlation approximation, after Ref. 26. This allows us to map the original interacting-spin problem onto one of non-interacting pseudospins, at the expense of neglecting correlations between different flip-flop transitions (see Appendix C). Such approximation is justified roughly for times smaller than the characteristic time scales of the flip-flop process, i.e., $t<1/A_{\max}^{(i,e)}$ (see Table I).

IV. INHOMOGENEOUS BROADENING

In free-induction decay experiments performed on molecular ensembles, the progressive dephasing of the different spins results in the decay of the average transverse magnetization, $\langle\sigma_{x,y}^{\mathcal{S}}\rangle \propto |r(t)|$. Besides dispersion in the molecule parameters (e.g., the g factor), such inhomogeneous broadening is due to local fluctuations in the Overhauser field (i.e., to the different quantum states of the nuclear environment felt by each replica of $\mathcal{S}$). This is theoretically accounted by a mixed $\rho_{\mathcal{E}}$. In Fig. 2, we show the time evolution of the decoherence factor: Each black curve refers to an initial density operator $\rho_{\mathcal{E}}(0)=\Sigma_{i=1}^{n} p_{\alpha_i}|\mathbf{I}_{\alpha_i}\rangle\langle\mathbf{I}_{\alpha_i}|$ (with $p_{\alpha_i}=1/n$ and $n=100$), with randomly generated values of α_i.[27] If all the Cr atoms have spinless nuclei [panel (a)], a smooth, approximately Gaussian decay of $|r(t)|$ takes place within 10^2 ns, with no critical dependence on the initial state of the nuclear spins. The fact that dispersion in the Overhauser field is entirely responsible for decoherence on this time scale is confirmed by the comparison with the case where the electron-nuclear Ising couplings in H' are omitted [$\omega_p^{(e)}=0$, straight blue line], where no appreciable decay takes place. The substitution of a spinless Cr with a ^{53}Cr isotope ($I_{\mathrm{Cr}}=3/2$) introduces a larger energy scale in the nuclear dynamics, corresponding to the contact hyperfine interaction at the corresponding site (see Table I). A major difference with respect to the previous case is marked by the occurrence of rapid oscillations [panel (b)]. These essentially result from the two specific contributions, which are separately shown in the figure inset. Their characteristic frequencies are clearly determined by $|I_{\mathrm{Cr}}^z|$, whereas

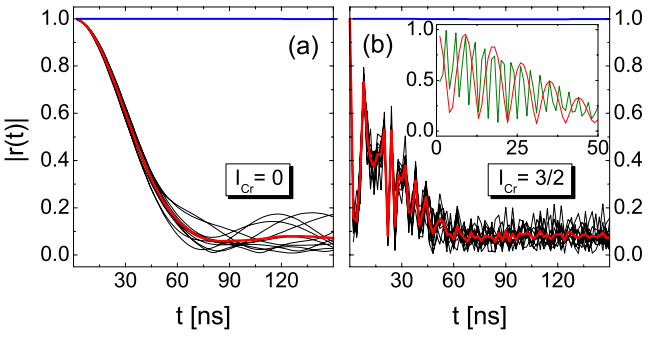

FIG. 2. (Color online) Time evolution, in modulus, of the decoherence factor r. Each solid black line corresponds to an average over 10^2, randomly generated, initial states of the nuclear bath. The red curves represent the average over the black ones. (a) All the Cr ions in the molecule have spinless nuclei. (b) The Cr ion opposite to Ni in the octahedron (see Fig. 1) has spin $I=3/2$. Same set of initial conditions and same magnetic field $B=1$ T, as in (a). Inset: Initial states corresponding to $I_{\mathrm{Cr}}^z=\pm 3/2$ (green) and $I_{\mathrm{Cr}}^z=\pm 1/2$ (red) are considered separately.

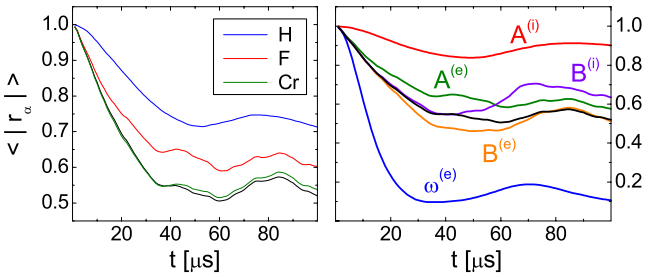

FIG. 3. (Color online) (a) Time evolution of $\langle|r_\alpha|\rangle$ as a function of the chemical composition: no substitutions (black curve); the spinless Cr opposite to Ni is substituted by a $I=3/2$ isotope (green); all the F nuclear spins are replaced by spinless atoms (red), or the H by ^{2}H (blue). (b) Time evolution of $\langle|r_\alpha|\rangle$ obtained with the full Hamiltonian H' (black curve), and after turning off each of the terms specified in the panel (colored curves). All the curves are averaged over the same set of $n=100$ initial nuclear states.

no sensible dependence on the initial state of the remaining nuclei shows up. Also, in this case, the time evolution of r is driven by the electron-nuclear Ising terms in H': In fact, for $\omega_p^{(e)}=0$ the decay of the decoherence factor is frozen [straight blue line, panel (b)]. Therefore, the overall density matrix on these time scales is approximately given by

$$\rho_{\mathcal{SE}}(t)=\sum_\alpha p_\alpha|\mathbf{I}_\alpha\rangle\langle\mathbf{I}_\alpha|\otimes|\psi_{\mathcal{S}}^\alpha(t)\rangle\langle\psi_{\mathcal{S}}^\alpha(t)|,$$

with $|\psi_{\mathcal{S}}^\alpha(t)\rangle=(e^{i\Delta_\alpha t}|\Uparrow\rangle+e^{-i\Delta_\alpha t}|\Downarrow\rangle)/\sqrt{2}$ and $\Delta_\alpha=\Sigma_{p=1}^{N_n}\omega_p^{(e)}I_p^z(\alpha)+\Sigma_{p\leqslant q}B_{p,q}^{(e)}I_p^z(\alpha)I_q^z(\alpha)$. As a consequence, the decoherence factor is $r(t)\simeq\Sigma_\alpha p_\alpha e^{2i\Delta_\alpha t}$. According to the above expression, no electron-nuclear entanglement takes place on the nanosecond time scale. We incidentally note that this is in general not the case if the nuclei are initialized in a pure state, consisting of a linear superposition of different configurations.[28] For example, if $|\psi_{\mathcal{E}}(0)\rangle=\Sigma_\alpha p_\alpha^{1/2}|\mathbf{I}_\alpha\rangle$, then $r(t)\simeq\Sigma_{\alpha,\beta}(p_\alpha p_\beta)^{1/2}e^{i(\Delta_\alpha+\Delta_\beta)t}$ and $\rho\neq\rho_{\mathcal{S}}\otimes\rho_{\mathcal{E}}$.

V. ELECTRON-NUCLEAR ENTANGLEMENT

The degree of purity of the molecule state is limited by the entangling of $\mathcal{S}$ and $\mathcal{E}$, even in the absence of dispersion in the Overhauser field. In fact, for an initial density matrix $\rho(0)=|\psi_{\mathcal{S}}\rangle\langle\psi_{\mathcal{S}}|\otimes|\mathbf{I}_\alpha\rangle\langle\mathbf{I}_\alpha|$, the phase coherence between the states $|\Uparrow\rangle$ and $|\Downarrow\rangle$ is reduced by the nuclear flip-flop transitions, which results in a diverging evolution of the states $|\mathbf{I}_\alpha^{\Uparrow}(t)\rangle$ and $|\mathbf{I}_\alpha^{\Downarrow}(t)\rangle$. In order to factor out such contribution in the more general case of a mixed nuclear state, we consider $\langle|r_\alpha(t)|\rangle=\Sigma_\alpha p_\alpha|r_\alpha|$: With a slight abuse of language, we refer to this expression as "average electron-nuclear entanglement," where the average is performed over the nuclear-spin configurations.[29] The above average does not in general correspond to any observable quantity, apart from the spin echo time, where the effect of inhomogeneous broadening is canceled out, and $\langle|r_\alpha(t)|\rangle$ coincides with the decoherence factor. As shown in Fig. 3, the characteristic time scale of the time decay is now tens of microseconds [panel (a), black curve].

In order to gain a deeper insight into the underlying dynamics, we isolate the role played by the different chemical elements. This analysis also has a practical relevance, since selective substitutions in Cr_7Ni have already been demonstrated.[18] Unlike inhomogeneous broadening, the effectiveness of electron-nuclear entanglement is only moderately affected by the introduction of a Cr isotope (green line). The substitution of the F nuclei with spinless ones and that of the H with ^{2}H (red and blue lines, respectively) result instead in a relevant increase, on average, of $|r_\alpha(t)|$. In panel (b), we compare the evolution of $\langle|r_\alpha(t)|\rangle$ obtained with the full effective Hamiltonian [black curve, same as in panel (a)], with those obtained after turning off different terms in H'. The most striking changes correspond to the cases of the intrinsic off-diagonal terms [$A_{p,q}^{(i)}=0$, red] and the extrinsic diagonal ones [$\omega_p^{(e)}=0$, blue]. While in the former case the average electron-nuclear entanglement is practically suppressed, in the former it is strongly increased with respect to the values obtained with the full Hamiltonian H'. The dependence of $\langle|r_\alpha(t)|\rangle$ on the $\omega_p^{(e)}$ can be possibly explained as follows: These corrections to the nuclear Zeeman frequencies, being in general different from nucleus to nucleus, tend to put out of resonance flip-flop transitions between otherwise identical elements, thus slowing down the nuclear dynamics. The dependence of $\langle|r_\alpha(t)|\rangle$ on the other intrinsic and extrinsic terms in H' (green, orange, and purple curves) is less remarkable. In a technological perspective, this suggests that the effectiveness of the magnetic field as a means to further suppress decoherence is saturated at high magnetic fields. In fact, the extrinsic couplings $A_{p,q}^{(e)}$ and $B_{p,q}^{(e)}$, which scale like Ω^{-1}, can be suppressed by increasing the field ($\Omega\propto B$); however, this does not seem to affect drastically electron-nuclear entanglement. On the other hand, the intrinsic terms $A_{p,q}^{(i)}$, which are mainly responsible for this effect, are independent of the field. Further results on the magnetic-field dependence of the electron-spin decoherence are provided in the next section.

VI. SPIN ECHO

The electron coherence can be partially recovered by applying suitable spin-echo sequences.[18,30–32] In the following, we investigate the creation and decay of the molecule coherence under the effect of an idealized Hahn-echo sequence, $\pi/2-\tau-\pi-\tau-$echo. In particular, each pulse is assumed to be instantaneous as compared with the nuclear time scales. Besides, we neglect coherences eventually generated by the π pulse between different nuclear states.[33,34] More specifically, the first $\pi/2$ pulse is assumed to create an in-plane polarization, initializing the molecule's electron spin to $|\psi_{\mathcal{S}}\rangle=(|\Downarrow\rangle+|\Uparrow\rangle)/\sqrt{2}$. The π pulse, instead, swaps $|\Uparrow\rangle$ and $|\Downarrow\rangle$ at time $t=\tau$. Therefore, immediatly after the pulse ($t=\tau$),

$$|\psi_{\mathcal{SE}}^\alpha(\tau_+)\rangle=\sigma_x^{\mathcal{S}}|\psi_{\mathcal{SE}}^\alpha(\tau_-)\rangle$$
$$=[|\Downarrow\rangle\otimes|\mathbf{I}_\alpha^{\Uparrow}(\tau_-)\rangle+|\Uparrow\rangle\otimes|\mathbf{I}_\alpha^{\Downarrow}(\tau_-)\rangle]/\sqrt{2},$$

where $\rho_{\mathcal{SE}}(t)=\Sigma_\alpha p_\alpha|\psi_{\mathcal{SE}}^\alpha(t)\rangle\langle\psi_{\mathcal{SE}}^\alpha(t)|$, and τ_+ (τ_-) is the time immediately after (before) the pulse. In other words, for $\tau<t<2\tau$, the evolution of the nuclear states $|\mathbf{I}_\alpha^\eta(t)\rangle$ is no longer induced by H', as for $0<t<\tau$, but rather by a Hamiltonian where $H_n^{(e)}$ is replaced by $-H_n^{(e)}$. In Fig. 4, we show

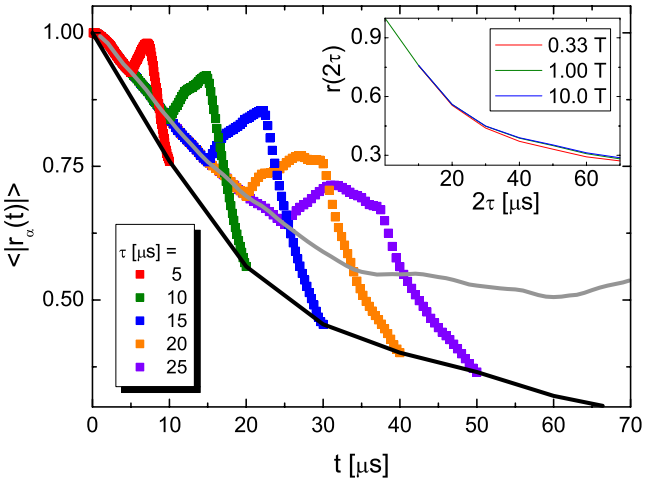

FIG. 4. (Color online) Time evolution of $\langle|r_\alpha|\rangle$, for $0 \leqslant t \leqslant 2\tau$ and $B=1$ T, after the application of an instantaneous π pulse at different times τ (colored lines). The black curve corresponds to $\langle|r_\alpha(t=2\tau)|\rangle$, whereas the gray one gives $\langle|r_\alpha(t)|\rangle$ in the absence of spin echo. Inset: $r(t=2\tau)$ for different values of the static field B.

the time dependence of $\langle|r_\alpha(t)|\rangle$, during the time interval $[0,2\tau]$, for different values of τ. This shows the effect of the π pulse on the average electron-nuclear entanglement. Besides, $\langle|r_\alpha(t)|\rangle$ coincides with an observable quantity (it is proportional to the transverse magnetization) for $t=2\tau$, where the effect of inhomogeneous broadening is completely reversed and $|r(t)|$ is very close to $\langle|r_\alpha(2\tau)|\rangle$ (see black curve and figure inset). For all the considered values of τ, the π pulse produces a partial disentanglement, denoted by the increase of $\langle|r_\alpha(t)|\rangle$ for $t>\tau$. This reaches a maximum at $t \sim \tau\sqrt{2}$,[31] and drops at later times (colored squares). In fact, for $t=2\tau$, the degree of electron-nuclear entanglement (not the overall decoherence, which is also affected by inhomogeneous broadening) is higher than it would be in the absence of spin echo (gray curve). The disentanglement is more effective (i.e., the maximum of $\langle|r_\alpha(t)|\rangle$ is higher) for smaller values of τ. The occurrence of a maximum disentanglement at a time earlier than the classical spin-echo time 2τ results from the interplay between invertible (e) and noninvertible (i) contributions, with roughly the same magnitude (Table I). The dependence of the electronic polarization at $t=2\tau$ is very well approximated by an exponential decay $e^{-\alpha t}$, with $1/\alpha = 19.8$ μs. However, we stress that the underlying dynamics is not a Markovian one. We finally consider the effect of the static magnetic field B (figure inset). While a finite B reduces the efficiency of relaxation processes, its increase within the considered range of values does not lead to a further suppression of decoherence (see also Fig. 3 and related discussion).

VII. CONCLUSIONS

In conclusion, we have theoretically investigated the effect of hyperfine interactions on the electronic coherence of a single Cr_7Ni molecule. Dispersion in the Overhauser field is shown to act on a time scale of $\sim$10 ns and to be qualitatively affected by the possible presence of Cr isotopes. H and F nuclei, instead, are mainly responsible for the average electron-nuclear entanglement, with a rate of ~ 0.1 μs^{-1}. Spin echo leads to a substantial cancellation of both effects, but at different time delays. Finally, neither of the two decohering mechanisms can be completely suppressed by large magnetic fields.

ACKNOWLEDGMENTS

The authors acknowledge stimulating discussions with W. A. Coish, D. Klauser, and D. Loss. This work has been carried out within the framework of the EU Network of Excellence "MAGMANet" Contract No. 515767, and supported by MIUR under PRIN No. 2006029518 and FIRB Contract No. RBIN01EY74.

APPENDIX A: ELECTRON-NUCLEAR-SPIN HAMILTONIAN

We model the single Cr_7Ni molecule as a collection of electron and nuclear spins. The positions of the latter are derived by x-ray diffraction analyses. The $N_n=152$ magnetically active nuclei correspond to the 144 H, with spin $I_H=1/2$, and to the 8 F nuclei ($I_F=1/2$). Where specified, we also consider the presence of a Cr isotope, with spin $I_{Cr}=3/2$. The electron spins are accounted for by $N_e=8$ electronic multiplets, localized on top of the Cr and Ni ions ($s_{Cr}=3/2$, $s_{Ni}=1$). The dominant direct coupling between these nuclei is given by the dipole-dipole interaction: $H_{nn}^{dip}=\sum_{p=1}^{N_n}\sum_{q=1}^{p-1}h_{nn}^{dip}(\mathbf{I}_p,\mathbf{I}_q)$. In terms of the rising and lowering operators, the dipolar terms read ($\hbar=1$)

$$h_{nn}^{dip}(\mathbf{I}_p,\mathbf{I}_q) = \frac{\gamma_p^l\gamma_q^l}{r_{pq}^3}[\mathbf{I}_p\cdot\mathbf{I}_q - 3(\mathbf{I}_p\cdot\hat{\mathbf{r}}_{pq})(\mathbf{I}_q\cdot\hat{\mathbf{r}}_{pq})] \equiv \sum_{\alpha,\beta=z,\pm} E_{pq}^{\alpha\beta} I_p^\alpha I_q^\beta,$$

where $\mathbf{r}_{pq}=\mathbf{r}_p-\mathbf{r}_q$ is the relative position of nuclei p and q, and the coefficients $E_{pq}^{\alpha\beta}$ are given by the following expressions:

$$E_{pq}^{zz} = \frac{\gamma_p^N\gamma_q^N}{r_{pq}^3}(1-3\cos^2\theta_{pq}),$$

$$E_{pq}^{-+} = \frac{1}{4}\frac{\gamma_p^N\gamma_j^N}{r_{pq}^3}(3\cos^2\theta_{pq}-1),$$

$$E_{pq}^{+z} = -\frac{3}{2}\frac{\gamma_p^N\gamma_q^N}{r_{pq}^3}\sin\theta_{pq}\cos\theta_{pq}e^{-i\varphi_{pq}},$$

$$E_{pq}^{++} = -\frac{3}{4}\frac{\gamma_i^N\gamma_q^N}{r_{pq}^3}\sin^2\theta_{pq}e^{-2i\varphi_{pq}}.$$

Besides, $E_{pq}^{-z}=[E_{pq}^{+z}]^*$ and $E_{pq}^{--}=[E_{pq}^{++}]^*$. Here, r_{pq}, θ_{pq}, and φ_{pq} give the relative position of the particles in spherical coordinates. An analogous expression apply to the electron-nuclear dipole-dipole interaction (in the point-dipole approximation):

$H_{en}^{dip}=\Sigma_{p=1}^{N_e}\Sigma_{q=1}^{N_n}h_{en}^{dip}(\mathbf{I}_p,\mathbf{s}_q)$. The dipole-dipole interactions between electron spins (H_{ee}^{dip}) are already included in the effective spin Hamiltonian, which is diagonalized to obtain the eigenstates $|\Uparrow\rangle$ and $|\Downarrow\rangle$.[16]

We then rewrite the electron-nuclear dipole-dipole Hamiltonian H_{en}^{dip} in the basis of the electron-spin eigenstates, and project it onto the ground-state doublet,

$$H_{en}^{dip}=\mathbb{P}_{1/2}\sum_{p=1}^{N_e}\sum_{q=1}^{N_n}\frac{\gamma_p^e\gamma_q^n}{r_{pq}^3}[\mathbf{s}_p\cdot\mathbf{I}_q-3(\mathbf{s}_p\cdot\hat{\mathbf{r}}_{pq})(\mathbf{s}_q\cdot\hat{\mathbf{r}}_{pq})]\mathbb{P}_{1/2}$$
$$\equiv\sum_{q=1}^{N_n}\sum_{\alpha,\beta=z,\pm}D_q^{\alpha\beta}\sigma_\alpha^{\mathcal{S}}I_q^\beta,$$

where $\mathbb{P}_{1/2}=|\Downarrow\rangle\langle\Downarrow|+|\Uparrow\rangle\langle\Uparrow|$, $\sigma_-^{\mathcal{S}}=|\Downarrow\rangle\langle\Uparrow|$, $\sigma_+^{\mathcal{S}}=|\Uparrow\rangle\langle\Downarrow|$, and $\sigma_z^{\mathcal{S}}=|\Uparrow\rangle\langle\Uparrow|-|\Downarrow\rangle\langle\Downarrow|$. The coefficients that enter the expression of the dipole-dipole couplings now include the matrix elements of the localized electron spins in the basis $\{|\Uparrow\rangle,|\Downarrow\rangle\}$,

$$D_q^{zz}=2\sum_{p=1}^{N_e}\frac{\gamma_p^e\gamma_q^N}{r_{pq}^3}\langle\Uparrow|s_p^z|\Uparrow\rangle(1-3\cos^2\theta_{pq}),$$

$$D_q^{-+}=\frac{1}{2}\sum_{p=1}^{N_e}\frac{\gamma_p^e\gamma_q^N}{r_{pq}^3}\langle\Downarrow|s_p^-|\Uparrow\rangle(3\cos^2\theta_{pq}-1),$$

$$D_q^{+z}=-\frac{3}{2}\sum_{p=1}^{N_e}\frac{\gamma_p^e\gamma_q^N}{r_{pq}^3}\langle\Uparrow|s_p^+|\Downarrow\rangle\sin\theta_{pq}\cos\theta_{pq}e^{-i\varphi_{pq}},$$

$$D_q^{++}=-\frac{3}{4}\sum_{p=1}^{N_e}\frac{\gamma_p^e\gamma_q^N}{r_{pq}^3}\langle\Uparrow|s_p^+|\Downarrow\rangle\sin^2\theta_{pq}e^{-2i\varphi_{pq}}.$$

Finally, $D_q^{-z}=[D_q^{+z}]^*$ and $D_q^{--}=[D_q^{++}]^*$.

APPENDIX B: EFFECTIVE NUCLEAR HAMILTONIAN

In order to discuss the derivation of the effective nuclear Hamiltonian H', it is convenient to divide the spin Hamiltonian $H=H_e+H_n+H_{en}$ into three parts: H_0, which corresponds to the only-electron terms and to the nuclear Zeeman ones; H_1, which inlcudes H_{nn}^{dip} and all the terms in H_{en} that are diagonal in the basis $\{|\Uparrow\rangle,|\Downarrow\rangle\}$; H_2, which groups the off-diagonal electron-nuclear terms in H_{en},

$$H_0=H_e+H_n^Z,$$

$$H_1-H_{nn}^{dip}=\sum_{\eta=\Uparrow,\Downarrow}|\eta\rangle\langle\eta|H_{en}|\eta\rangle\langle\eta|$$
$$=\sigma_z^{\mathcal{S}}\sum_{p=1}^{N_n}[(a_p/2+D_p^{zz})I_p^z+D_p^{+z}I_p^++D_p^{-z}I_p^-],$$

$$H_2=H_{en}-\sum_{\eta=\Uparrow,\Downarrow}|\eta\rangle\langle\eta|H_{en}|\eta\rangle\langle\eta|$$
$$=\sigma_+^{\mathcal{S}}\otimes\sum_{p=1}^{N_n}[D_p^{+z}I_p^z+D_p^{++}I_p^++(a_p+D_p^{-+})I_p^-]+\text{H.c.}$$

The effective Hamiltonian H' results from the following canonical transformation:

$$\bar{H}=WHW^{-1}=e^SHe^{-S}\simeq H+[S,H]+\frac{1}{2!}[S,[S,H]]$$
$$=H_0+H_1+[S,H_1+H_2]+[S,[S,H_1+H_2]-H_2]/2$$
$$\simeq H_0+H_1+([S,H_2]/2),$$

where S is such that $[S,H_0]=-H_2$. Only the terms that commute with $\sigma_z^{\mathcal{S}}$ and $I_T^z=\Sigma_{p=1}^{N_n}I_p^z$, and are up to second order in $D_q^{\alpha\beta}$, are retained. The expression of $S=\Sigma_{p=1}^{N_n}S_p$ is given in Sec. III.

The effective Hamiltonian finally reads

$$H'=(\Omega^r/2)\sigma_z^{\mathcal{S}}+H_n^{(i)}+\sigma_z^{\mathcal{S}}\otimes H_n^{(e)}.$$

The intrinsic and extrinsic effective nuclear Hamiltonians read

$$H_n^{(\chi)}=\sum_{p=1}^{N_n}\omega_p^{(\chi)}I_p^z+\sum_{p\neq q}A_{p,q}^{(\chi)}I_p^+I_q^-+\sum_{p\leqslant q}B_{p,q}^{(\chi)}I_p^zI_q^z,$$

with $\chi=i,e$. The coefficients entering the expression of $H_n^{(i)}$ are given by

$$\omega_p^{(i)}=\omega_p+\frac{1}{\Omega}[|a_p+D_p^{-+}|^2+D_p^{++}D_p^{--}],$$

while $A_{p,q}^{(e)}=E_{pq}^{+-}$ and $B_{p,q}^{(e)}=E_{pq}^{zz}$. The coefficients entering the expression of $H_n^{(e)}$ are given by

$$A_{p,q}^{(e)}=\frac{1}{\Omega}[(a_p+D_p^{-+})(a_q+D_q^{+-})+D_p^{++}D_q^{--}+\text{c.c.}],$$

$$B_{p,q}^{(e)}=\frac{1}{\Omega}(D_p^{+z}D_q^{-z}+D_p^{-z}D_q^{+z}),$$

while $\omega_p^{(e)}=a_p/2+D_p^{zz}$. Finally, the interaction with the nuclear spins renormalizes the electron Zeeman splitting,

$$\Omega^r=\Omega+\frac{2}{\Omega}\sum_{p=1}^{N_n}[|a_p+D_p^{-+}|^2+D_p^{++}D_p^{--}].$$

APPENDIX C: NUCLEAR DYNAMICS

We describe the system dynamics in terms of N_{ps} pseudospins, one for each possible flip-flop transition between a pair of nuclear spins.[26] In this representation, the overall state of the nuclear bath is specified by that of the N_{ps} pseudospins,

$$|\mathbf{I}_\alpha^\eta(t)\rangle=\otimes_{p=1}^{N_n}|\phi_p^\eta(t;\alpha)\rangle\leftrightarrow|\Psi_\alpha^\eta(t)\rangle=\otimes_{k=1}^{N_{ps}}|\psi_k^\eta(t)\rangle,$$

where $\eta=\Uparrow,\Downarrow$. Here, the initial conditions corresponding to the spin configuration α are given by $|\phi_p^\eta(0;\alpha)\rangle=|I_p^z(\alpha)\rangle$ and

$|\psi_k^\eta(0)\rangle \equiv |\uparrow_k\rangle$. Therefore, the pseudospin $k(p,q)$ is oriented downward (upward) if (no) flip-flop transitions between the nuclear spins p and q take place. Each pseudospin k evolves independently of one another (pair-correlation approximation) according to the following equation: $|\psi_k^\eta(t)\rangle = e^{-i\mathcal{H}_k^\eta t}|\uparrow_k\rangle$, where $\mathcal{H}_k^\eta = \mathbf{h}_k^\eta \cdot \sigma_k/2$. Here, the pseudomagnetic field $\mathbf{h}_k^\eta$ can be expressed as follows in terms of the effective nuclear-spin Hamiltonian H': $h_{k,x}^{\Uparrow/\Downarrow} = \langle I_p^z, I_q^z | H' | I_p^z - 1, I_q^z + 1\rangle/2$ and $h_{k,z}^{\Uparrow/\Downarrow} = \langle I_p^z, I_q^z | H' | I_p^z, I_q^z\rangle - \langle I_p^z - 1, I_q^z + 1 | H' | I_p^z - 1, I_q^z + 1\rangle$. This results in

$$h_{k,x}^{\Uparrow/\Downarrow} = \prod_{\xi=p,q} [(I_\xi + \alpha_\xi I_\xi^z)(I_\xi - \alpha_\xi I_\xi^z + 1)]^{1/2} [A_{p,q}^{(i)} \pm A_{p,q}^{(e)}]/2$$

and

$$h_{k,z}^\eta = \sum_{\chi=i,e} \alpha_\eta^{(\chi)} \Bigg\{ [\omega_p^{(\chi)} - \omega_q^{(\chi)}] + B_{p,q}^{(\chi)}(1 + I_q^z - I_p^z) + \sum_{m\neq p,q} [B_{p,l}^{(\chi)} - B_{q,l}^{(\chi)}] I_l^z - \sum_{l=p,q} B_{l,l}^{(\chi)}(1 - 2I_l^z) \Bigg\},$$

where $\alpha_{p/q} = \pm 1$, $\alpha_\eta^{(i)} = 1$, and $\alpha_{\Uparrow/\Downarrow}^{(e)} = \pm 1$.

For each initial configuration of the nuclear bath, the decoherence factor is therefore given by

$$r(t) = \prod_{k=1}^{N_{ps}} \langle \psi_k^\Downarrow(t) | \psi_k^\Uparrow(t)\rangle \equiv \prod_{k=1}^{N_{ps}} r_k(t).$$

Here, the contribution of each pseudospin is given by $r_k(t) = \langle \psi_k^\Downarrow(t) | \psi_k^\Uparrow(t)\rangle$. This corresponds to

$$r_k(t) = \langle \uparrow_k | \exp\{i\sigma \cdot \hat{n}^\Downarrow \phi^\Downarrow t/2\} \exp\{-i\sigma \cdot \hat{n}^\Uparrow \phi^\Uparrow t/2\} | \uparrow_k \rangle$$

with

$$\phi^\eta = [(h_{k,x}^\eta)^2 + (h_{k,z}^\eta)^2]^{1/2}, \quad n_{x/z}^\eta = \frac{h_{k,x/z}^\eta}{\phi^\eta}, \quad n_y^\eta = 0.$$

We also compute the evolution of the decoherence factor under the effect of the Hahn-echo sequence. In this case, the π pulse instanteneously swaps the electron-spin states $|\Uparrow\rangle$ and $|\Downarrow\rangle$ at $t = \tau$. The state of the pseudospin k corresponding to an initial state $\Uparrow$ of the electron spin is thus given by

$$|\psi_k^{\Uparrow\Downarrow}(t > \tau)\rangle = \exp\{-i\mathcal{H}_k^\Downarrow (t - \tau)\} \exp\{-i\mathcal{H}_k^\Uparrow \tau\} |\uparrow_k\rangle.$$

The contribution of each pseudospin to the decoherence factor is correspondingly given by $r_k(t > \tau) = \langle \psi_k^{\Downarrow\Uparrow}(t) | \psi_k^{\Uparrow\Downarrow}(t)\rangle$. This corresponds to

$$r_k(t > \tau) = \langle \psi_k^\Downarrow(\tau) | \exp\{i\sigma \cdot \hat{n}^\Uparrow \phi^\Uparrow (t - \tau)/2\} \times \exp\{-i\sigma \cdot \hat{n}^\Downarrow \phi^\Downarrow (t - \tau)/2\} | \psi_k^\Uparrow(\tau)\rangle.$$

*troiani.filippo@unimore.it

[1] D. Giulini, E. Joos, C. Kiefer, J. Kupsch, I.-O. Stamatescu, and H. D. Zeh, *Decoherence and the Appearence of a Classical World in Quantum Theory* (Springer-Verlag, Berlin, 1996).

[2] W. H. Zurek, Rev. Mod. Phys. **75**, 715 (2003).

[3] M. Schlosshauer, Rev. Mod. Phys. **76**, 1267 (2004).

[4] M. A. Nielsen and I. L. Chuang, *Quantum Computation and Quantum Information* (Cambridge University Press, Cambridge, 2000).

[5] N. V. Prokof'ev and P. C. E. Stamp, Rep. Prog. Phys. **63**, 669 (2000).

[6] J. Lehmann, A. Gaita-Ariño, E. Coronado, and D. Loss, Nat. Nanotechnol. **2**, 312 (2007).

[7] F. Troiani, U. Hohenester, and E. Molinari, Phys. Rev. Lett. **90**, 206802 (2003).

[8] V. Cerletti, W. A. Coisch, O. Gywat, and D. Loss, Nanotechnology **16**, R27 (2005).

[9] F. Meier, J. Levy, and D. Loss, Phys. Rev. B **68**, 134417 (2003).

[10] S. Carretta, P. Santini, G. Amoretti, F. Troiani, and M. Affronte, Phys. Rev. B **76**, 024408 (2007).

[11] F. K. Larsen, E. J. L. McInnes, H. El Mkami, J. Overgaard, S. Piligkos, G. Rajaraman, E. Rentschler, A. A. Smith, G. M. Smith, V. Boote, M. Jennings, G. A. Timco, and R. E. P. Winpenny, Angew. Chem., Int. Ed. **42**, 101 (2003).

[12] J.-P. Cleuziou, W. Wernsdorfer, V. Bouchiat, T. Ondarcuhu, and M. Monthioux, Nat. Nanotechnol. **1**, 53 (2006).

[13] A. Cornia, A. C. Fabretti, M. Pacchioni, L. Zobbi, D. Bonacchi, A. Caneschi, D. Gatteschi, R. Biagi, U. Del Pennino, V. De Renzi, L. Gurevich, and H. S. J. Van der Zant, Angew. Chem., Int. Ed. **42**, 1645 (2003).

[14] V. Corradini, R. Biagi, U. del Pennino, V. D. Renzi, A. Gambardella, M. Affronte, C. A. Muryn, G. A. Timco, and R. E. P. Winpenny, Inorg. Chem. **46**, 4937 (2007).

[15] F. Troiani, M. Affronte, S. Carretta, P. Santini, and G. Amoretti, Phys. Rev. Lett. **94**, 190501 (2005).

[16] F. Troiani, A. Ghirri, M. Affronte, S. Carretta, P. Santini, G. Amoretti, S. Piligkos, G. Timco, and R. E. P. Winpenny, Phys. Rev. Lett. **94**, 207208 (2005).

[17] E. Micotti, Y. Furukawa, K. Kumagai, S. Carretta, A. Lascialfari, F. Borsa, G. A. Timco, and R. E. P. Winpenny, Phys. Rev. Lett. **97**, 267204 (2006).

[18] A. Ardavan, O. Rival, J. J. L. Morton, S. J. Blundell, A. M. Tyryshkin, G. A. Timco, and R. E. P. Winpenny, Phys. Rev. Lett. **98**, 057201 (2007).

[19] A. Morello, P. C. E. Stamp, and I. S. Tupitsyn, Phys. Rev. Lett. **97**, 207206 (2006).

[20] V. Bellini, A. Olivieri, and F. Manghi, Phys. Rev. B **73**, 184431 (2006).

[21] G. Breit, Phys. Rev. **35**, 1447 (1930).

[22] S. Blugel, H. Akai, R. Zeller, and P. H. Dederichs, Phys. Rev. B **35**, 3271 (1987).

[23] N. Shenvi, R. de Sousa, and K. B. Whaley, Phys. Rev. B **71**, 224411 (2005).

[24] W. A. Coish and D. Loss, Phys. Rev. B **72**, 125337 (2005).

[25] W. M. Witzel, R. de Sousa, and S. Das Sarma, Phys. Rev. B **72**, 161306(R) (2005).

[26] W. Yao, R.-B. Liu, and L. J. Sham, Phys. Rev. B **74**, 195301 (2006).

[27] A systematic exploration of the nuclear Hilbert space is beyond the scope of the present work. Hereafter, we have therefore com-

pared different sets of initial conditions, besides those reported. There, no sensible changes in the dynamics show up, and neither do results from a further increase of n.

[28] F. M. Cucchietti, J. P. Paz, and W. H. Zurek, Phys. Rev. A **72**, 052113 (2005).

[29] In the present case, this is equivalent to considering the difference between the von Neumann and the Shannon entropies (Ref. 4), $S(\rho_S)-H(\mathbf{p}_\alpha)=\langle S(\rho_\alpha)\rangle$.

[30] W. A. Coish and D. Loss, Phys. Rev. B **70**, 195340 (2004).

[31] W. Yao, R.-B. Liu, and L. J. Sham, Phys. Rev. Lett. **98**, 077602 (2007).

[32] B. V. Fine, Phys. Rev. Lett. **94**, 247601 (2005).

[33] Such coherences are responsible for the modulations observed in electron-spin echo envelope modulation experiments (Refs. 18 and 34). Therefore, no such modulations show up in the present simulations.

[34] A. Schweiger and G. Jeschke, *Principles of Pulse Electron Paramagnetic Resonance* (Oxford University Press, New York, 2001).

[35] V. Corradini, F. Moro, R. Biagi, U. del Pennino, V. De Renzi, S. Carretta, P. Santini, M. Affronte, J. C. Cezar, G. Timco, and R. E. P. Winpenny, Phys. Rev. B **77**, 014402 (2008).